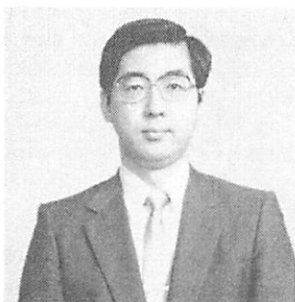


STABILITY AND MEASUREMENT IN CONCRETE FAILURE

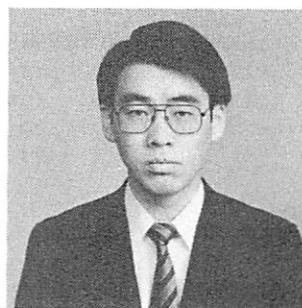
(Reprint from Transactions of JCI, Vol.5, 1983)



Wataru KOYANAGI



Keitetsu ROKUGO



Yuichi UCHIDA

SYNOPSIS

The relation between the controlling method of testing and the stability of fracture phenomena was investigated. Complete load-displacement curves of concrete specimens were measured with an ordinary (not stiff) testing machine. An abrupt fracture of the specimens was restrained by monitoring the speed of a pen on the X-Y recording chart. Cylindrical specimens ( $\phi 10 \times 20$  cm) of high strength concrete in compression ( $\sigma_c = 1123 \text{ kgf/cm}^2$ ) and beam specimens ( $10 \times 10 \times 40$  cm) of resin concrete in flexure ( $\sigma_b = 190 \text{ kgf/cm}^2$ ) showed a peculiar region, where both load and displacement decreased on load-displacement curves after strength failure.

---

W. Koyanagi is professor of civil engineering at Gifu University, Gifu, Japan. He received his Doctor of Engineering Degree in 1977 from Kyoto University. He and his coauthors were awarded for this paper in 1983 from JCI. His research interests cover fracture properties of concrete material, reinforced concrete members and structures, structural design method and the use of new building materials. He is a member of ACI, JSCE, JSMS, and JCI.

---

K. Rokugo is associate professor of civil engineering at Gifu University. He received his Doctor of Engineering Degree in 1980 from Kyoto University. His research interests include the evaluation and improvement of toughness of concrete materials and reinforced concrete members. He is a member of ACI, JSCE, JSMS, and JCI.

---

Y. Uchida is a research engineer at Research Institute of Shimizu Construction Co., LTD, Tokyo, Japan. He received his Master of Engineering Degree in 1983 from Gifu University, where this investigation was carried out. His current research interests include the strength performance of lapped splices in reinforced concrete and the bond resistance of reinforcement. He is a member of JSCE and JCI.

---

## STABILITY AND MEASUREMENT IN CONCRETE FAILURE

Wataru KOYANAGI<sup>\*</sup>, Keitetsu ROKUGO<sup>\*</sup> and Yuichi UCHIDA<sup>\*\*</sup>

### ABSTRACT

In case of concrete specimens and reinforced concrete members, even if displacement rate during tests is controlled with a stiff testing machine, the fracture phenomena after strength failure become often unstable. In such a case, it is impossible to measure complete load displacement curves including the descending portion. The purpose of this paper is to establish general methods to obtain complete load displacement curves of concrete specimens. The following results were obtained. Complete load-displacement curves of concrete specimens were measured with an ordinary (not stiff) testing machine by operating oil valves and were recorded in X-Y recording chart. That is, an abrupt increase in dissipating energy, which corresponded to fracture of the specimens, was restrained by monitoring the speed of a pen on the X-Y recording chart. For resin concrete specimens, an increase in dissipating energy could be also restrained by monitoring the rate of acoustic emissions. Cylindrical specimens ( $\phi 10 \times 20$ cm) of high strength concrete in compression ( $\sigma = 1123 \text{ kgf/cm}^2$ ) and beam specimens ( $10 \times 10 \times 40$ cm) of resin concrete<sup>c</sup> in flexure ( $\sigma_b = 190 \text{ kgf/cm}^2$ ) showed a peculiar region, where both load and displacement decreased on load-displacement curves after strength failure. In case of beam specimens of mortar, the longer the span length, the clearer the appearance of the peculiar region.

### INTRODUCTION

New type concretes reinforced with steel fiber or glass fiber have been developed to improve mainly the toughness of concrete. The term "toughness" means the energy absorbing capacity of materials or structural members at failure, i.e. total work done. To evaluate the toughness of the materials and members, complete load-displacement relationship including so-called falling branch or descending portion after strength failure, i.e. after the maximum load, must be obtained.

---

\* Department of Civil Engineering, Gifu University

\*\* Shimizu Construction Co. LTD

In testing brittle concrete-like materials, even if the displacement rate is controlled by stiff testing machine during loading, the fracture phenomena after the maximum load often become unstable. This makes it impossible to obtain complete load-displacement curves including the descending portion.

The purpose of this study is to establish the general method of measuring for the complete load-displacement curves of concrete specimens. At first, relation between the stability of fracture phenomena and the controlling method of loading were studied. The effects of the length change of the elastic uncracked portions of beam specimens on the load-displacement relations were theoretically and experimentally examined. In addition, fracture characteristics of various concretes under flexure as well as compression were compared with each other using the load-displacement curves obtained by the established measuring method.

## 1. STABILITY OF FRACTURE PHENOMENA AND LOAD-DISPLACEMENT RELATIONS

### 1.1. STABILITY IN FRACTURE AND LOAD CONTROLLING METHOD

In order to discuss the stability of fracture phenomena of concrete like materials, typical load-displacement curves, i.e. Curve A and Curve B, are presented in Fig. 1. Owing to the facts that the stresses of concrete specimen can not be obtained accurately in flexure and actual stresses and strains in concrete specimens are far from uniform even in simple uniaxial compressive loading[1], load-displacement relations are adopted as a generalized expression in stead of stress-strain relations. The displacement is defined here as that of the specimen in the direction of loading at the loading point. The definition is considered to be very convenient to analyze the fracture phenomena by energy concept because the applied energy on the specimen can be easily calculated from the area under the obtained load-displacement curves. The effect of three types of loading on the fracture phenomenon is discussed as follows.

#### a) Control of loading rate

When the load increasing rate is kept constant during loading, the points on the load axis after the strength failure do not correspond one to one to the points on both Curves A and B. Therefore, unstable fracture occurs at the peak load point (a and b on Curves A and B,

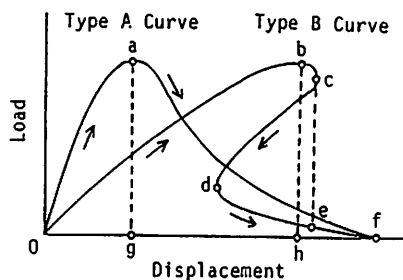


Fig. 1. Two Types of Load-Displacement Curve.

respectively), and the portion of curves after the strength failure can not be recorded.

b) Control of displacement rate

When the displacement increasing rate is kept constant, the points on the displacement axis correspond one to one to the points on Curve A but not on Curve B. Thus, Curve A can be recorded completely, but Curve B cannot. In case of Curve B, under the constant displacement rate, discontinuous (catastrophic) transfer from point c to point e in Fig. 1 must have occurred. Therefore, the portion of the curve c-d-e after point c cannot be measured.

Now the relations between the stiffnesses of the testing machine and a specimen are dealt with. Total displacement of the machine-specimen system is the sum of displacements of the two. When the load-displacement relation of the specimen belongs to the type A curve in Fig. 1 and the stiffness of the testing machine  $K_m$  is higher than the absolute maximum value of negative stiffness of the specimen  $|K_s|_{\max}$  (in case of  $K_{m1}$  in Fig. 2), the relation between the load and the total displacement of the combined machine-specimen system also shows the type A curve as shown in Fig. 2(c). In this case, complete load-displacement curve can be obtained by controlling the displacement rate. Though the load-displacement relation of the specimen belongs to type A, when the stiffness of the testing machine  $K_m$  is lower than  $|K_s|_{\max}$  (in case of  $K_{m2}$  in Fig. 2), the relation of load versus total displacement of the combined system shows the type B curve. In this case, complete load-displacement curves cannot be obtained by the displacement rate control test.

When the load-displacement relation of the specimen belongs to the type B Curve, complete load-displacement curves cannot be obtained by controlling the displacement rate test as far as the rate is non-negative, even how higher the machine stiffness is. In order to obtain the relation completely in such a case, not only the displacement but also the load must be lowered after the peak load has been attained.

c) Control of fracture rate

To obtain the complete load-displacement relations of the

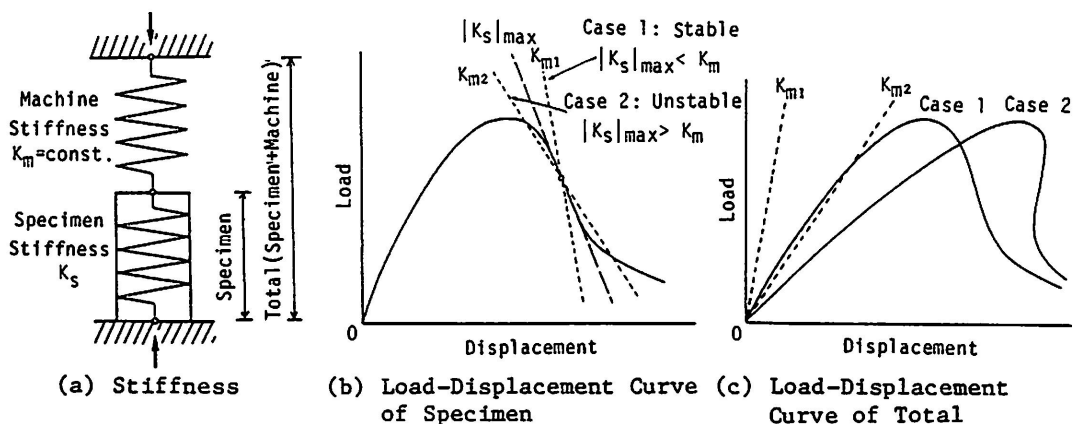


Fig. 2. Stability of Fracture of Specimen.

specimens with type B curve, or of the case of  $K_m < |K|_{s, \max}$ , catastrophic fracture must be prevented. Due to the decrease both in load and displacement after the strength failure, the rate of the fracture phenomena corresponding to the points on the curve one to one should be chosen as the control parameters in stead of load or displacement rate. One of the most appropriate control parameters is considered to be the amount of dissipating energy which corresponds to the degree of fracture[2].

### 1.2. PREVIOUS RESEARCH ON THE LOAD CONTROLLING METHOD

Several studies have been reported on the complete stress-strain relations rather than load-displacement relations of various concrete specimens under compressive loading. The relations were obtained by controlling the displacement test, and they belong to type A curve in Fig. 1. The stiffness of the testing machine was increased by the adoption of stiffening support or servo-control system. The tests were always made on the standard specimens ( $h/d=2$ ). Complete stress-strain curves of high strength concrete specimens more than  $800 \text{ kgf/cm}^2$  were reported[3]. Researchs on the load-displacement curve which belongs to type B in Fig. 1 have been made few on concrete but several on rocks by Fairhurst and others[4][5][6]. The control parameters they had chosen were crack opening distance (COD) in flexural test and deformation in perpendicular to the axial force in compression test.

### 1.3. SPECIMEN SIZE AND LOAD-DISPLACEMENT CURVES

The effect of the specimen size on the load-displacement curve of concrete in flexure was examined. In a flexural test of concrete a main crack develops rapidly after peak load has been attained[2]. The beam specimen except for the main crack region is considered to remain elastic because few internal cracks are generated after the peak load has been attained except for the main crack region. Accordingly, displacement of beam specimen, i.e. deflection, after the peak load ( $\delta_t$ ) consists of two components. One is the deflection caused by the rotation of the main crack region ( $\delta_\theta$ ), and the other is caused by the elastic deformation of uncracked region ( $\delta_e$ ). Two kinds of flexural specimens A and B are shown

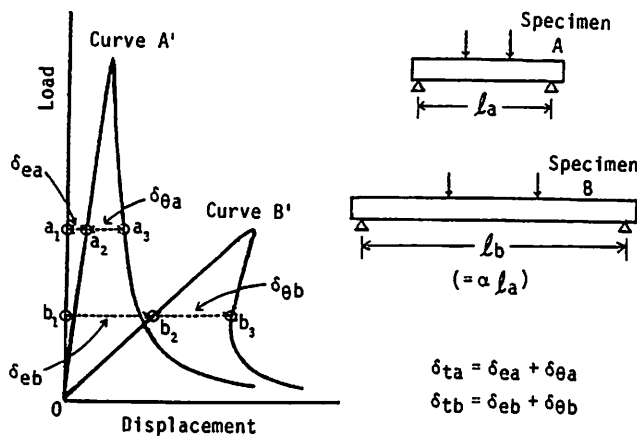


Fig. 3. Effect of Span Length on Load-Displacement Curve.

in Fig. 3. These specimens have a same cross section and different span lengths of  $l_a$  and  $l_b (= l_a \alpha)$  for specimens A and B, respectively. Load-displacement curves under a third point loading of specimens A and B are denoted as A' and B', respectively, and illustrated in Fig. 3. The displacement is defined here as an average of deflections at the loading points. Draw a line to the curve A' parallel to displacement axis in Fig. 3 at a certain load level, say  $1/\beta$  of the maximum load. Take points  $a_1$ ,  $a_2$  and  $a_3$  on the line, which are the intersecting points on the load axis, in the increasing part and in the decreasing part of the curve A', respectively. Total displacement  $\delta_{ta}$  can be expressed by the sum of the displacement due to elastic deformation  $\delta_{ea} (= a_1a_2)$  and due to the rotation at the cracked region  $\delta_{\vartheta a} (= a_2a_3)$ . Similarly, draw a line to the curve B' at the same load level, i.e.  $1/\beta$  of the maximum load. Points  $b_1$ ,  $b_2$  and  $b_3$  on the line represent also the intersecting point on the load axis, in the increasing part and descending part of curve B', respectively. Displacements due to elastic deformation  $\delta_{eb}$  and due to crack rotation  $\delta_{\vartheta b}$  correspond to  $b_1b_2$  and  $b_2b_3$ , respectively. As the rotation at the cracked region is generated by a flexural moment, it is assumed that the length of a main crack and the amount of rotation under the same flexural moment are all the same, though the span length is different. Accordingly, there exist the following relations between  $\delta_{ea}$  and  $\delta_{eb}$ , and  $\delta_{\vartheta a}$  and  $\delta_{\vartheta b}$ , which correspond to each other at the same loading level to the maximum load in their load-displacement curves.

$$\delta_{ea} = \delta_{eb} / \alpha^2 \quad (1)$$

$$\delta_{\vartheta a} = \delta_{\vartheta b} / \alpha \quad (2)$$

When the span length of a specimen with a certain cross section increases, not only the load carrying capacity but also the displacement decrease after the peak load has been attained, e.g. curve B' shown in Fig. 4. The reason of such a fracture phenomena is explained as follows. Though the span length of the specimen increases, length of fracture region and the total dissipating energy which is needed to break the specimen remains constant. However, when the span length increases, uncracked portion of the specimen increases and elastic strain energy accumulated in that portion also increases. When the elastic strain energy at the peak load becomes large enough to break the specimen, the load-displacement curve changes from type A' to type B'. The evidence is proved experimentally and will be discussed in the next session.

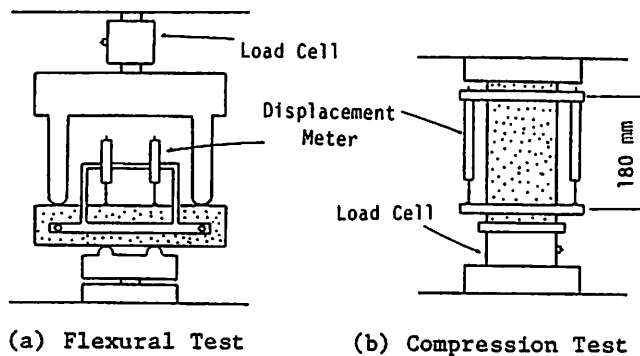


Fig. 4. Test Setup.

## 2. MEASUREMENT OF LOAD-DISPLACEMENT CURVES

### 2.1. TEST PROGRAM

The complete load-displacement curves of concrete specimens under flexure were measured and effects of the span length on the shape of the curve were investigated. Third point loading was made on mortar flexural specimens with various span lengths and complete load-deformation curves were obtained, which include Type B curves in Fig. 1. As stated above, since type B curve can not be obtained by a stiff testing machine alone, a testing method with the control of fracture rate was adopted.

Mortar mix proportion was fixed at W:C:S = 0.5:1.0:3.0, and an average compressive strength of standard specimens was 442 kgf/cm<sup>2</sup>. The cross section of the specimens was 7.5×7.5 cm. Three kinds of specimen lengths and also three kinds of span lengths were selected, i.e. 35, 70 and 100 cm and 30, 60 and 90 cm, respectively. Five specimens were made for each test. The specimens were stored in water at 20°C and tests were made at the age of 14 days.

Third point loading were made manually by conventional Amsler type testing machine of 200 tonf in capacity, where an oil driving valve and an oil returning valve were provided. Neither automatic electro mechanical servo-controlled system nor so-called stiff testing machine were adopted. Deflections at both of the loading points were measured by two strain gage type displacement meters as shown in Fig.4. The deflections obtained were averaged and load-displacement relations were recorded in X-Y recoring chart.

### 2.2. CONTROL OF FRACTURE PHENOMENA

In a flexural fracture process of concrete, a single or a few number of cracks start on the tension face of the specimens. Because of the crack propagation toward the compression side, the specimens lose their load carrying capacity. It is known that the dissipating energy is proportional to the fracture degree, that is, the crack propagation in concrete specimens in flexure[2]. The dissipating energy is indicated by the area bounded by the loading and unloading curves in the load-displacement diagrams.

In this study, the dissipating energy was used as the control parameter. The catastrophic fracture of the specimens was avoided and was controlled by restraining the rate of the dissipating energy. Actually, moving speed of a pen on an X-Y recorder was monitored and was controlled.

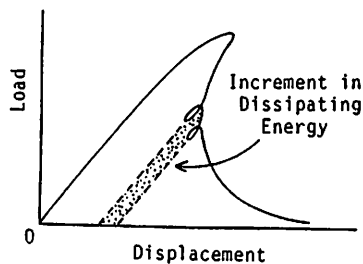


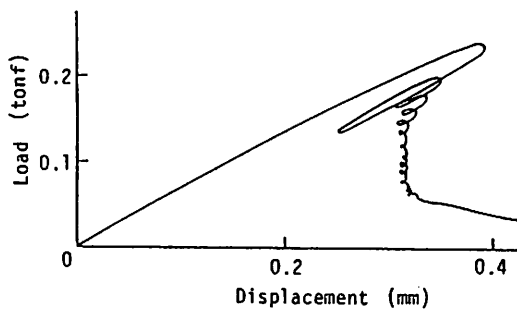
Fig. 5. Increment in Dissipating Energy.

After the peak load has been attained and when load decrement was observed, oil return valve was opened appropriately and unloading was made slightly. Thus the pen speed was restricted not to increase abruptly. The loading and unloading were repeated until the specimens became final fracture. The increment of the dissipating energy is represented by the hatched area shown in Fig. 5. Since the pen speed relates to the rate of the dissipating energy, the rate of fracture was controlled by the pen speed.

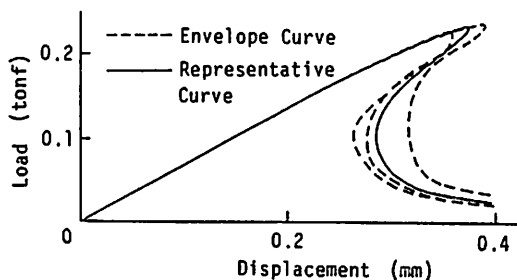
### 2.3. LOAD-DISPLACEMENT CURVE UNDER FLEXURE

Fig. 6(a) shows an example of a crude load-displacement curve of a flexural specimen. In order to restrain the abrupt increase of the dissipating energy, loading-unloading operation was repeated after the peak load was attained. Three to five envelope load-displacement curves were used to obtain the averaged curve for each loading condition as graphically shown in Fig. 6(b). Curves shown with dotted lines are the obtained envelope curves while a curve with full line is the averaged representative load-displacement curve under the corresponding test condition. The latter is called merely as the load-displacement curve hereafter.

The load-displacement curves of three kinds of mortar specimens are illustrated with full line in Fig. 7. Their span lengths were 30, 60 and 90 cm. When the span length becomes longer, such a tendency becomes remarkable that not only the load but also the displacement decrease. The



(a) Example of Measured Load-Displacement Curve



(b) Envelope Curves and Representative Curve.

Fig. 6. Measured Load-Displacement Curves.



descending parts of the curve for the span length of 30 and 90 cm are estimated from the curve for the span length of 60 cm by Eq. (2) and represented in Fig. 7 with dotted lines. The calculated curves coincide with their full line curves fairly well. The fact proves that the considerations stated in the previous article on the specimen size and the load-displacement curve are correct.

Flexural strength  $\sigma_b$ , applied energy at the peak load  $W_p$  and total dissipating energy  $W_f$  of three kinds of specimens are obtained from the load-displacement curves, and the averages are listed in Table 1. Applied energy at the peak load  $W_p$  can be obtained from the area bounded by the curve oag for Curve A or obg for Curve B and a displacement axis as shown in Fig. 1. Dissipating energy  $W_f$  can be obtained similarly to the curve oaf for Curve A or obcdef for Curve B. Corrected flexural strength  $\sigma_b'$ , where the effect of its own weight is taken into account, is also tabulated in Table 1.

When the span length increases, flexural strength  $\sigma_b'$  and dissipating energy  $W_f$  decrease. However, the decrements are slight. The effect of the span length on the flexural strength and the dissipating energy is considered to be small. Applied energy at the peak load  $W_p$ , however, increases largely with the increase of the span length. For the specimens of 90 cm in span length, the applied energy  $W_p$  exceeds the dissipating energy  $W_f$ . In this case, more amount of energy is accumulated in a specimen than that is needed to break the specimen at the point of the peak load. If the loading is controlled by displacement rate, the specimen becomes unstable after the peak load has been attained, and catastrophic fracture occurs at the moment. In other words, energy  $W_p$  already stored in the specimen will be transformed into the energy  $W_f$  to break the specimen, and the rest ( $W_p - W_f$ ) will be transformed into kinetic energy which makes the specimen to scatter.

In spite of the increase of the span length, rupture of the specimens occurs only in a limited portion and the dissipating energy  $W_f$  which is needed to break the specimens remains almost constant. On the other hand, applied energy  $W_p$  increases with the increase of the span length, because the length of the elastic zone which can accumulate the elastic strain

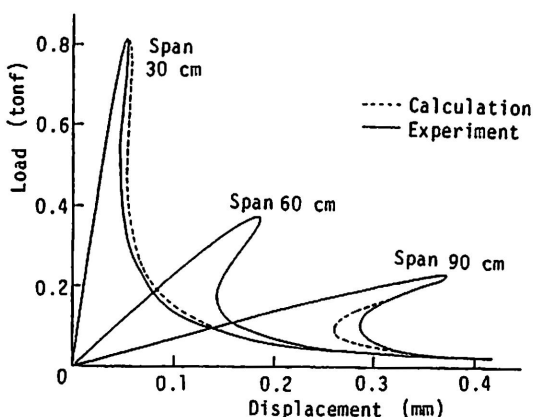


Fig. 7. Load-Displacement Curves of Mortar Specimens.

energy increases. It is why such a phenomenon become remarkable when the loading span becomes longer that the displacement as well as the load decrease on the load-displacement curve after the maximum load has been attained, and the fracture phenomenon becomes unstable.

### 3. COMPARISON OF FRACTURE BEHAVIOR OF VARIOUS CONCRETES

Various types of concretes have been developed recently. In order to know and to compare the mechanical properties and fracture behavior of the concretes, it is convenient to use the complete load-displacement relations of specimens of same size. Complete load-displacement curves under compression as well as flexure of four kinds of concrete were obtained and the fracture behaviors were examined.

#### 3.1. TEST PROGRAM

Four kinds of concrete were tested. They were high strength concrete (denoted as series H), steel fiber reinforced high strength concrete (series HF), polyester resin concrete (series R) and ordinary plain concrete (series P).

In series H and HF, superplasticizer (Pz NL-4000) was used. Steel fiber used in series HF was plate shear cut type fiber of 0.5×0.5×30 mm (aspect ratio : 75). Fiber content in series HF was 2.0 percent by volume. In series R, unsaturated polyester resin was used as the binder of aggregate instead of cement paste.

The size of specimens for flexural test was 10×10×40 cm, and that for compression test was 10×20 cm. All the specimens except for series R were cured in water at 21°C for 7 days and then in moist room at 21°C for 21 days. Loading tests were made at the age of 28 days.

Displacement in compression was measured by the compressometer shown in Fig. 4(b), which was attached directly to the specimen. Gage length of the compressometer was 18.0 cm. The loading method and the measurement of displacement in the flexural test was all the same as that described in 2.2. The compressive and flexural strengths of the four concretes are summarized in Table 2.

#### 3.2. LOAD-DISPLACEMENT CURVE UNDER COMPRESSION TESTS

The obtained load-displacement curves of the four kinds of concrete specimens under compression are illustrated in Fig. 8. To obtain the complete load-displacement curve for high strength concrete (series H) after peak load, the controlling method described in 2.2. was employed

Table 1. Test Results of Mortar Specimens.

Span (cm)	Flexural Strength (kgf/cm <sup>2</sup> )		Dissipating Energy (kgf·cm)	
	$\sigma_b$	$\sigma_b'$	$W_p$	$W_f$
30	58.0	58.2	2.1	4.9
60	53.6	54.4	3.7	4.4
90	50.1	52.0	4.6	4.2

which restrained the abrupt increase of dissipating energy. Even in the compression test, such a phenomenon was also observed that both the displacement and load decreased after peak load. There are few reports on the complete load-displacement curve or complete stress-strain curve of such a high compressive strength concrete of more than  $1000 \text{ kgf/cm}^2$ . The decrement of the curve after the peak load for high strength concrete specimens is so steep that it is quite difficult to obtain the displacement by the ordinarily displacement control type stiff testing machine.

The inclination of the decrement of the curve of series P and series HF after the peak load were more gradual than that of series H. When the inclination was small, the curve may be obtained by the controlling the rate of displacement and without using the loading-unloading cyclic method.

The effect of the steel reinforcement on the energy dissipation at compression fracture can be evaluated by the difference in the enclosed areas of the curve of series H and series HF. Not only high strength but also high toughness concrete can be manufactured with steel fiber reinforcement for ordinary high strength concrete. In comparison of the curves of series P and series H, the compressive strength of high strength concrete shows 2.5 times as much as that of ordinary concrete, whereas toughness of the former at the compression fracture shows only 1.5 times as much as that of the latter.

### 3.3. LOAD-DISPLACEMENT CURVE UNDER FLEXURAL TESTS

Obtained load-deformation curves of the four kinds of concrete specimens under flexure are given in Fig. 9. In order to avoid the abrupt increase of the dissipating energy at the test, fracture rate was controlled by restraining the speed of the recording pen as described in 2.2. In series R, it can be clearly seen that there is a region where both load and displacement decrease in the curve. In case of resin concrete specimen, in addition to the above controlling method, count

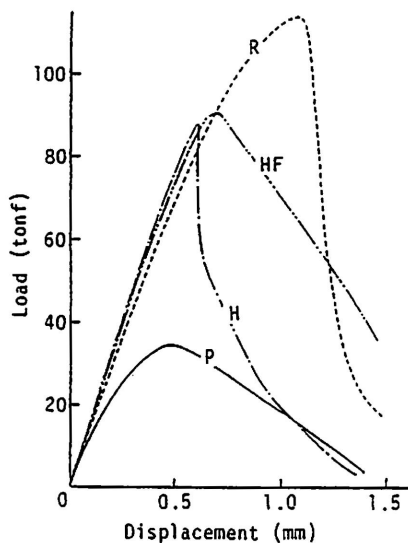


Fig. 8. Compressive Load-Displacement Curves of Specimens.

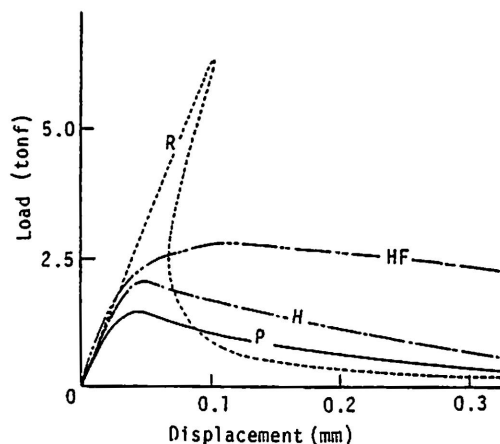


Fig. 9. Flexural Load-Displacement Curves of Specimens.

rate of generated acoustic emissions was also employed. The attenuation of acoustic emissions in resin concrete was smaller in comparison with that in cement concrete, because the former does not have gel structure which the latter has. That is why the count rate of acoustic emission for resin concrete is more than ten times as much as that for cement concrete at the same sensitivity. In the tests of cement concrete, count rate of the acoustic emission was so small that it could not be used as a fracture rate control parameter. In the flexural test of resin concrete specimens, the load was monotonously increased up to near the maximum load. Then the loading-unloading operations were repeated not to increase the count rate of the acoustic emission abruptly.

Total dissipating energy  $W_f$  to rupture the flexural specimen was calculated from the enclosed area by the curves and listed in Table 2. By the way, Fig. 9 shows only the displacement within 0.3 mm. The displacement at the rupture was so large that it could not be given in the Figure. Total dissipating energy to rupture the specimen in flexure remarkably increases when steel fiber was mixed with high strength concrete. The flexural strength of resin concrete is much higher than ordinary concrete or high strength concrete, however, total dissipating energy at rupture of resin concrete is almost the same as that of the latter.

Load-displacement relations after the peak load under flexure are considered to be governed by the relation between the flexural strength and the total dissipating energy to rupture. On the other hand, the maximum decrement slope of the curve under compression seems steeper when the strength ratio of  $\sigma_c/\sigma_b$  becomes larger. More research is needed on the shape of load-displacement curve of various concrete in terms of strength characteristics, the strength ratio and the energy dissipation characteristics.

## CONCLUSIONS

The purpose of this study was to establish the general method for measuring the complete load-displacement curves of concrete including the region after peak load. The relation between the controlling method of testing and the stability of fracture phenomena was investigated. Flexural tests of mortar specimens with various span length were carried to confirm the considerations on the shape of the curves. Flexural and compressive loading on various concrete were also made, and the shapes of the curves were compared. Principal conclusions derived are as follows;

Table 2. Test Results of Various Types of Concretes.

Kinds of Concrete	Compressive Strength (kgf/cm <sup>2</sup> ) $\sigma_c$	Flexural Strength (kgf/cm <sup>2</sup> ) $\sigma_b$	Dissip. Energy of Whole Beam (kgf·cm) $W_f$
Ordinary Plain Concrete(P)	455	44.6	30
High Strength Concrete (H)	1123	62.3	49
Steel Fiber Reinforced High Strength Concrete (HF)	1165	84.9	226
Resin Concrete (R)	1480	190	30

(1) In order to obtain the complete load-displacement curve of concrete specimens under flexure as well as compression, the catastrophic fracture due to the decrease of both load and displacement after the strength failure must be avoided. For this purpose, appropriate control parameters which correspond to the points on the curve one to one should be chosen instead of load or displacement control only. It is not necessary to employ the stiff testing machine for measuring the curve when the appropriate control parameter is adopted and the oil returning valve provided is operated well.

(2) The amount of dissipating energy is considered to be the most appropriate control parameter, because it directly corresponds to the degree of fracture. In this study, the catastrophic fracture of the specimens was avoided and was controlled by restraining the rate of the dissipating energy. Actually, moving speed of a pen on an X-Y recorder was monitored and was controlled. Count rate of acoustic emissions was also monitored to control the rate of dissipating energy in the test of resin concrete.

(3) It was theoretically estimated and experimentally proved that there is the region where both load and displacement decrease after the peak load on the complete load-displacement curve. The phenomenon became remarkable when the span length increased. The fact was explained by the energy balance in a specimen and the curve with various span length were well estimated.

(4) Four kinds of concrete were tested under flexure as well as compression. The region on the curve stated above was clearly observed in the test of high strength concrete specimens under compression ( $\phi 10 \times 20$  cm,  $\sigma_c = 1123$  kgf/cm<sup>2</sup>) and in the test of resin concrete specimens under flexure ( $70 \times 10 \times 40$  cm,  $\sigma_b = 190$  kgf/cm<sup>2</sup>). The phenomenon cannot be observed when an ordinary stiff testing machine is employed and the rate of displacement is controlled.

(5) When steel fiber was mixed with high strength concrete, not only high strength but also high toughness concrete was obtained. The effectiveness of steel fiber on the energy dissipation at fracture was calculated by the difference of the area between the curve of series HF and that of series H.

#### REFERENCES

- (1) Dantu, P., "Etude des contraintes dans les milieux heterogenes. Application du beton," Annales de l'Institut Technique du Batiment et des Travaux Publics, V.11, N.121, pp.55-77, Jan., 1958. (in French)
- (2) Okada, K., W. Koyanagi and K. Rokugo, "Energy Approach on the Fracture Process of Concrete in Flexure," Proc. Japan Society of Civil Engineers, No. 285, pp.109-119, May 1979. (in Japanese)
- (3) Hiramatsu, Y. et al. "Designing and Constructing a Stiff Testing Machine and the Deformation Characteristics of Various Kinds of Concrete," Jour. Society of Materials Science, Japan., V.24, No.260, pp.447-454, May 1975. (in Japanese)
- (4) Hardy, M.P., J.A. Hudson and C. Fairhurst, "The Failure of Rock Beams Part 1 - Theoretical Studies," Int. Jour. Rock Mech. Min. Sci., V.10, pp.53-67, 1973.
- (5) Hudson, J.A., M.P. Hardy and C. Fairhurst, "The Failure of Rock Beams Part 2 - Experimental Studies," *ibid.* pp.69-82
- (6) Hudson, J.A., S.L. Crouch and C. Fairhurst, "Soft, Stiff and Servo Controlled Testing Machines, A Review with Reference to Rock Failure," Dept. of Civil and Mineral Eng., Univ. of Minnesota, 1971.